

Article

Solution of Moore–Gibson–Thompson Equation of an Unbounded Medium with a Cylindrical Hole

Ahmed E. Abouelregal ^{1,2} , Hakan Ersoy ³  and Ömer Civalek ^{4,5,*} 

¹ Department of Mathematics, College of Science and Arts, Jouf University, Al-Qurayyat 75911, Saudi Arabia; ahabogal@mans.edu.eg

² Department of Mathematics, Faculty of Science, Mansoura University, Mansoura 35516, Egypt

³ Division of Mechanics, Department of Mechanical Engineering, Akdeniz University, Antalya 07058, Turkey; hakanersoy@akdeniz.edu.tr

⁴ Division of Mechanics, Department of Civil Engineering, Akdeniz University, Antalya 07058, Turkey

⁵ Research Center for Interneural Computing, China Medical University, Taichung 40447, Taiwan

* Correspondence: civalek@yahoo.com or omer@mail.cmuh.org.tw

Abstract: In the current article, in the presence of thermal and diffusion processes, the equations governing elastic materials through thermodiffusion are obtained. The Moore–Gibson–Thompson (MGT) equation modifies and defines the equations for thermal conduction and mass diffusion that occur in solids. This modification is based on adding heat and diffusion relaxation times in the Green–Naghdi Type III (GN-III) models. In an unbounded medium with a cylindrical hole, the built model has been applied to examine the influence of the coupling between temperature and mass diffusion and responses. At constant concentration as well as intermittent and decaying varying heat, the surrounding cavity surface is traction-free and is filled slowly. Laplace transform and Laplace inversion techniques are applied to obtain the solutions of the studied field variables. In order to explore thermal diffusion analysis and find closed solutions, a suitable numerical approximation technique has been used. Comparisons are made between the results obtained with the results of the corresponding previous models. Additionally, to explain and realize the presented model, tables and figures for various physical fields are presented.

Keywords: solution of thermoelastic diffusion; MGT equation; thermal and diffusion relaxation time; cylindrical hole



Citation: Abouelregal, A.E.; Ersoy, H.; Civalek, Ö. Solution of Moore–Gibson–Thompson Equation of an Unbounded Medium with a Cylindrical Hole. *Mathematics* **2021**, *9*, 1536. <https://doi.org/10.3390/math9131536>

Academic Editors: Theodore E. Simos and Charampos Tsitouras

Received: 28 May 2021

Accepted: 28 June 2021

Published: 30 June 2021

Publisher's Note: MDPI stays neutral with regard to jurisdictional claims in published maps and institutional affiliations.



Copyright: © 2021 by the authors. Licensee MDPI, Basel, Switzerland. This article is an open access article distributed under the terms and conditions of the Creative Commons Attribution (CC BY) license (<https://creativecommons.org/licenses/by/4.0/>).

1. Introduction

The theory of thermoelasticity has received a lot of interest from researchers and scientists due to its many applications in different fields. The fields of architecture, structural features, plasma physics, geophysics, aeronautics, missiles, steam turbine generators, etc. are among the most important areas in which this theory is used. For the first time, an uncombined principle of thermoelasticity was foreseen, in that the elastic strain is independent of the heat transfer and conversely. However, this hypothesis became invalid in displaying the practical results of many concrete problems. Then, researchers provided alternative theories of coupled thermoelasticity, which became widely known as a general thermoelastic theory. This concept has been gaining fame in recent years because its aim is to solve the contradiction of the unlimited heat propagation rate. This description, however, has become appropriate to some extent to communicate practical performance, such as high-speed energy transportation and low-temperature and high-heat transfer engineering.

The classical coupled thermoelasticity theory (CTE) [1] suggested by Biot expects a theoretically unrealistic unlimited velocity of the spread of heat. In order to remove the contradiction of the extraordinary physical phenomenon of unlimited speed in the CTE theory, non-classical thermoelasticity models known as generalized thermoelasticity have been formulated. Lord–Shulman [2], Green–Lindsay [3], and Green–Naghdi [4–6] theories

are major theories of generalized thermoelasticity that became the focus of current research in this field. Lord and Shulman [3] integrated the principle of heat flow rate into the law of Fourier with thermal relaxation time, and formulated a theory of extended thermoelasticity with a thermal flux rate. The energy equation as well as the relationship between Duhamel and Neumann were altered by Green and Lindsay [4], providing two relaxation periods. Theories of thermoelasticity without and with energy dissipation [4–6] have been proposed by Green and Naghdi. Roychoudhuri [7] suggested the three-phase-lag (TPL) thermoelastic model that involves three different phase delays in the heat flux vector, the gradient of temperature, and the gradient of thermal displacement function. The prevalent problems of thermoelasticity based on these new models are now of great significance [8–13].

The Moore–Gibson–Thompson Equation (MGT) has been heavily involved in a broad range of papers focused on study and understanding in recent decades. This concept stems from a differential equation of the third order, which is involved in the value of several dynamic fluid aspects [14]. Quintanilla [15] has built a new model of thermoelastic heat conduction (called “MGT thermoelasticity”) based on the Moore–Gibson–Thompson equation. Another new thermoelastic model with two temperatures, in which heat conduction was described as the historical MGT version, was given by Quintanilla [16], which emerged from the development of the theory of Green–Naghdi Type III by adding a relaxation factor. In the context of several mechanical aspects of the flux, this theory started with a third-order differential equation. The MGT thermoelastic model has led to a significant increase in the range of researchers devoted to this theory [17–30].

Diffusion is the transition from a higher concentration area to a less centered region (such as molecules, atoms, and ions). A mathematical relationship dependent on the concentration gradient defines diffusion. This phenomenon has resulted in several industrial purposes from the recent interest. In many fields, the diffusion concept is commonly used, including physics, economics, biology, sociology, chemistry, and finance. In bipolar transistor diffusion, integrated resistors are formed to form a base and emitter; spring/drain regions are formed in the MOS transistor, and dopes are formed in the MOS gated polysilicon transistor. Concentration is determined by what is called Fick’s Law in many of these areas of application. This is a basic law that does not deal with the interactions between the input substance and the medium in which the substance is incorporated or the effect of temperature on this reaction [31–33].

One of the distinguishing features of diffusion is that it depends on the spontaneous movement of particles, which, without the need for a direct mass movement, leads to mixing or mass transfer. One of the elements of approximation, or collective action, is a mass movement. The term “convection” describes the combination of two phenomena of transport. Temperature, contact zone, gradient steepness of concentration, and particle-size-effect diffusion. The rate and degree of diffusion can be adjusted independently and collectively by each factor. Entropy inequality is suggested for the blend and is used to restrict the constituent equations in a mixture of elastic materials subject to diffusion and thermal management. The constituents are later assumed to be isotropic solids and further restricted to the material frame–differentiation axiom and to reflect symmetrical conditions of the material. It is shown that the constituent functions can be written with respect to the left Cauchy–Green tensors for constituents.

Thermo-diffusion in solids, particularly metals, has been regarded as an unrelated amount of body deformation until recent times. Even so, a study demonstrates that the thermo-diffusing process can have a major impact on body deformation. The Thermoelastic diffusion concept was introduced by Nowacki [33–35]. The developed thermoelastic model was proposed in this concept. This requires propagation at infinite rates of thermoelastic waves. Sherief et al. [36] established a thermoelastic generalization theory suggesting limited spreading velocities for thermoelastic and propagating waves. In terms of the principle of generalized thermoelastic diffusion, Sherief and Saleh [37] and Sherief and Maghraby [38] have worked on a thermoelastic half-space issue with a permeating substance in contact with the bonding surface.

The thermo-diffusion theory and the combination of quasi-stationary diffusion problems for an elastic substrate have been investigated by several researchers [32,39–44]. The effects of cross-effects caused by the mixture of temperature, mass diffusion, and strain were studied, resulting in additional mass concentration due to thermal excitation and producing additional temperature ranges [45–50].

It was found from previous studies that the theory of the third form (GN-III) by Green and Naghdi has a similar defect as the usual Fourier model and also forecasts the immediate spread of thermal waves. Giorgi et al. [45] explained that such phenomena relevant to constant states are outside the control of the theory of Type III, which should be seen in Fourier as a principle of thermal conduction rather than as a simple theory. This theory is true for both stationary and sluggish thermal phenomena. To solve this dilemma, it is, therefore, natural to amend this suggestion. A new theory of thermal diffusion is formulated in this present work, in which the Moore–Gibson–Thompson equation defines the heat conduction and diffusion formulae. This model was designed to explore the interaction between elasticity, heat, and the mechanisms of diffusion of elastic materials that allow the propagation of thermal waves at finite rates. Many studies have been performed on the inversion of the Laplace transform in the literature [51–58]. More details for them will be given in the next sections. Indeed, the governing system equations can be realized in the new model after the addition of two relaxation factors in the GN-III model. Discrete singular convolution is also applied for some heat and cavity problems [59,60]. A modified and correct solution technique is proposed using the integral boundary formulations of the heat equation by Chernov and Reinarz [61].

The topic of thermo-diffusion interactions in an unbounded isotropic homogeneous solid with a cylindrical hole has been researched in the sense of the generalized model of Moore–Gibson–Thompson thermo-diffusion (MGT-TD). The surface of the cylinder is free of traction and, respectively, undergoes time-dependent convection and chemical load. By means of the Laplace transform method, an accurate solution to the issue is obtained first. The Laplace transformations have been reversed numerically. To show the diffusion effects and different physical phenomena of these solids, the study findings have also been numerically measured and graphically portrayed. Numerical values have been provided in figures and tables to illustrate the comparisons between the physical fields in order to allow a distinction between the results we obtained and the corresponding results in other special models.

2. The Basic MGT Thermo-Diffusion Equations

Many mathematicians, physicists, and engineers, as well as industry, widely use Fourier and Vic formulas to explain the thermal conductivity and diffusion in elastic materials. In this section, we will derive a new paradigm that allows describing the phenomena of heat transfer as well as propagation within materials in a manner consistent with the physical and chemical aspects.

In a homogeneous isotropic, elastic solids, the governing equations, and constitutive relationships for generalized thermo-diffusion behavior are established by [33–35]. The Fourier's law:

$$\mathbf{q}(x, t) = -K\nabla\theta(x, t) \quad (1)$$

The Fick's law:

$$\boldsymbol{\eta}(x, t) = -D\nabla P(x, t) \quad (2)$$

The strain–displacement relations:

$$e_{ij} = \frac{1}{2}(u_{j,i} + u_{i,j}) \quad (3)$$

The coupled conservation heat energy equation:

$$\rho C_e \frac{\partial \theta}{\partial t} + \beta_1 T_0 \frac{\partial}{\partial t}(\operatorname{div} \mathbf{u}) + a T_0 \frac{\partial C}{\partial t} = -\operatorname{div} \mathbf{q} + Q \quad (4)$$

The continuity equation [46]:

$$-\operatorname{div} \boldsymbol{\eta} = \dot{C} \quad (5)$$

The chemical potential P :

$$P = -\beta_2 e_{kk} + bC - a\theta \quad (6)$$

where heat flux \boldsymbol{q} , $\theta = T - T_0$ denotes the temperature increment in which T is the absolute temperature, T_0 is the reference temperature, K indicates the thermal conductivity, e_{ij} denotes the strain tensor and u_i is the displacement vector. Additionally, in Equations (1)–(6), P denotes the chemical potential, $\boldsymbol{\eta}$ denotes the flow of the diffusing mass vector, D is the diffusion coefficient, where $\operatorname{div} \boldsymbol{u} = e_{kk}$ is the cubical dilatation, Q is the source of heat, ρ is the density of the medium, C_e denotes the specific heat at constant strain, a is the measure of thermoelastic diffusion effect, C is the concentration of the diffusive material and $\beta_1 = (3\lambda + 2\mu)\alpha_t$ are the material constants (thermoelastic coupling), where α_t is the coefficient of the thermal expansion.

Although the elastic thermal diffusion laws of Fourier and Fick have been well tested for most practical problems, they do not specify a temporary short-time temperature area (higher frequencies and smaller wavelengths). We obtain parabolic partial differential equations through the combination of Equation (1) with (4) and (2) with (5). They emit an infinite velocity of propagation as a result. This property, from a physical point of view, conflicts with physical phenomena. In the past 3 decades, the non-classical diffusion and thermal elasticity theories have been replaced by more general equations to solve the previous inconsistency issue. The generalized model of thermo-diffusion with a time of relaxation was developed by Sherief et al. [36], which allows thermal wave propagation to be reduced.

In 1948, to solve the infinitely rapid propagation in the heat equation, Cattaneo proposed an updated equation for the heat equation. The relationship (1) was replaced by

$$\left(1 + \tau_0 \frac{\partial}{\partial t}\right) \boldsymbol{q}(x, t) = -K \nabla \theta(x, t) \quad (7)$$

where τ_0 is a thermal relaxation time parameter. Sherief et al. [36] postulated a similar mass flow equation in the same way and similar to Equation (7), given by:

$$\left(1 + \tau_1 \frac{\partial}{\partial t}\right) \boldsymbol{\eta}(x, t) = -D \nabla P(x, t) \quad (8)$$

where τ_1 indicates the diffusion time relaxation parameter. This ensures that the C equation also forecasts the limited velocity of spread of the substance from medium to media. This is achieved with concentration C .

The development of an alternative construction of heat diffusion was then suggested by Green and Naghdi [4–6] as an entirely new thermoelastic theory. The function ϑ is seen as a new constituent vector in the models of Green and Naghdi as a gradient of thermal displacement. In mechanical fields and in thermal fields, the scalar function ϑ is generally seen as the mechanical displacement equivalent. In addition, the function ϑ fulfills $\dot{\vartheta} = \dot{\theta}$. The law of improved thermal conductivity of the GN-III theory is described as [5]

$$\boldsymbol{q} = -K \nabla \theta(x, t) - K^* \nabla \vartheta(x, t) \quad (9)$$

In this instance, the parameter $K^* > 0$ is a constant material property and is also mentioned as the heat conductivity rate. Abouelregal [39,40] suggested a similar relation for the vector of heat flow to Equation (9) as:

$$\boldsymbol{\eta}(x, t) = -\nabla P(x, t) - D^* \nabla v(x, t) \quad (10)$$

In Equation (10), the chemical displacement rate v is regarded as a new constitutive variable in which parameter D^* is the diffusion rate factor. The chemical displacement function v satisfies the relation $\dot{v} = P$.

The combination of Fourier’s modified law (9) and energy Equation (4) has been found to lead to a series of elements in the point continuum, rendering the actual component infinitely dependent on the solutions. Equation (9) has the exact same flaw as the usual Fourier hypothesis that the waves of thermal conduction spread instantly. Therefore, this proposal was also generally updated, and Quintanilla [15,16] included a relaxation time to solve this problem, given the MGT equation. Quintanilla [15] made an adjustment to the proposed updated heat conduction equation (MGTE) after adding the relaxation factor in the Green–Naghdi form III model as follows:

$$\left(1 + \tau_0 \frac{\partial}{\partial t}\right) \mathbf{q} = -[K \nabla \theta + K^* \nabla \vartheta] \tag{11}$$

By differentiating Equation (11) and using the relationship $\dot{\vartheta} = \theta$, we have

$$\left(1 + \tau_0 \frac{\partial}{\partial t}\right) \dot{\mathbf{q}} = -\left(K \nabla \frac{\partial \theta}{\partial t} + K^* \nabla \theta\right) \tag{12}$$

As in Equation (11), the mass flux Equation (10) is assumed to be similar:

$$\left(1 + \tau_1 \frac{\partial}{\partial t}\right) \boldsymbol{\eta} = -[D \nabla P + D^* \nabla v] \tag{13}$$

After differentiating the previous relationship with respect to time and using $\dot{v} = P$, we obtain

$$\left(1 + \tau_1 \frac{\partial}{\partial t}\right) \dot{\boldsymbol{\eta}} = -\left[D \nabla \frac{\partial P}{\partial t} + D^* \nabla P\right] \tag{14}$$

By combining Equations (4) and (12), a modified type of heat conduction equation can be obtained, which is developed based on the MGTE equation [15,16]. When we take a divergence operator to Equation (12) and use Equation (4), we obtain:

$$\left(1 + \tau_0 \frac{\partial}{\partial t}\right) \left[\rho C_e \frac{\partial^2 \theta}{\partial t^2} + \beta_1 T_0 \frac{\partial^2 e}{\partial t^2} + a T_0 \frac{\partial^2 C}{\partial t^2} - \frac{\partial Q}{\partial t}\right] = K \nabla^2 \dot{\theta} + K^* \nabla^2 \theta \tag{15}$$

We also obtain the modified equation of mass diffusion by taking the divergence of Equation (15) and the use of Equations (5) and (6) as

$$\left(D \frac{\partial}{\partial t} + D^*\right) \left(b \nabla^2 C - \beta_2 \nabla^2 e_{kk} - a \nabla^2 \theta\right) = \left(1 + \tau_1 \frac{\partial}{\partial t}\right) \frac{\partial^2 C}{\partial t^2} \tag{16}$$

Complementing the system of equations that govern the behavior of thermal, dynamic, and diffusion propagation inside bodies with normal properties and homogeneity, we have [36]:

$$\mu u_{i,jj} + (\lambda + \mu) u_{j,ij} - \beta_1 \theta_{,i} - \beta_2 C_{,i} + F_i = \rho \ddot{u}_i \tag{17}$$

$$\sigma_{ij} = 2\mu e_{ij} + \delta_{ij} [\lambda e_{ij} - \beta_1 \theta - \beta_2 C] \tag{18}$$

where and β_2 is a material constant (diffusion coupling) given by $\beta_2 = (3\lambda + 2\mu)\alpha_c$, where α_c is the coefficient of the linear diffusion equation, σ_{ij} is the stress tensor, λ and μ are Lamé’s constants, and δ_{ij} is the Kronecker delta function.

Equation (15) occurs in viscous thermal soothing applications, with high intensity, medical and industrial applications such as ltuosis, thermal therapy, or ultrasound washing. The model is also known as the Kelvin or Zener model. This equation is found in the viscoelasticity theory, the classic linear viscoelastic model, to clarify the conduct of certain viscoelastic materials, including the complex and viscous micro-structures of fluids [48].

3. Implementation of the Proposed Model

We will study an infinitely homogeneous thermo-diffusive solid with a cylindrical hole of radius R and the boundary initially in a non-turbulent state and at a uniform temperature T_0 and an initial concentration of C_0 . We will use the cylindrical coordinate system (r, Θ, z) because of the nature of the problem, considering that the z -axis lies along the axis of the cylindrical hole. The state of a solid can be represented in terms of state r and time t variables because of the symmetry of the problem so that the values of all physical field variables vanish at infinity. We also assumed that there are no sources of external body force and heat that influence the body, implying that in the beginning, the body is calm.

The displacement and strain tensor components are given by

$$u_r = u(r, t), \quad u_\Theta = 0 = u_\varphi \tag{19}$$

$$e_{rr} = \frac{\partial u}{\partial r}, \quad e_{\Theta\Theta} = \frac{u}{r}, \quad e_{zz} = e_{rz} = e_{r\Theta} = e_{\Theta z} = 0 \tag{20}$$

Based on Equation (20), we can obtain the cubical dilatation as

$$e = e_{rr} + e_{\varphi\varphi} + e_{\Theta\Theta} = \frac{\partial u}{\partial r} + \frac{u}{r} \tag{21}$$

From Equations (6) and (18), the radial and hoop stresses and chemical potential can be written as

$$\sigma_{rr} = 2\mu \frac{\partial u}{\partial r} + \lambda e - \beta_1 \theta - \beta_2 C \tag{22}$$

$$\sigma_{\Theta\Theta} = 2\mu \frac{u}{r} + \lambda e - \beta_1 \theta - \beta_2 C \tag{23}$$

$$P = -\beta_2 e + bC - a\theta \tag{24}$$

The modified equations for MGT heat conduction (15) and MGTE mass diffusion (16) can be written as follows:

$$\left(1 + \tau_0 \frac{\partial}{\partial t}\right) \left[\rho C_e \frac{\partial^2 \theta}{\partial t^2} + \beta_1 T_0 \frac{\partial^2 e}{\partial t^2} + a T_0 \frac{\partial^2 C}{\partial t^2} - \frac{\partial Q}{\partial t}\right] = \left(K \frac{\partial}{\partial t} + K^*\right) \nabla^2 \theta \tag{25}$$

$$\left(D \frac{\partial}{\partial t} + D^*\right) \left(b \nabla^2 C - \beta_2 \nabla^2 e_{kk} - a \nabla^2 \theta\right) = \left(1 + \tau_1 \frac{\partial}{\partial t}\right) \frac{\partial^2 C}{\partial t^2} \tag{26}$$

where $\nabla^2 = \frac{\partial^2}{\partial r^2} + \frac{1}{r} \frac{\partial}{\partial r}$ is the cylindrical operator of Laplace. Equation (17) can be expressed as

$$\sigma_{rr,r} + \frac{1}{r}(\sigma_{rr} - \sigma_{\Theta\Theta}) = \rho \frac{\partial^2 u}{\partial t^2} \tag{27}$$

Inserting Equations (22) and (23) in Equation (27), we obtain

$$(\lambda + 2\mu) \left(\frac{\partial^2 u}{\partial r^2} + \frac{1}{r} \frac{\partial u}{\partial r} - \frac{u}{r^2}\right) - \left(\beta_1 \frac{\partial \theta}{\partial r} + \beta_2 \frac{\partial C}{\partial r}\right) = \rho \frac{\partial^2 u}{\partial t^2} \tag{28}$$

Multiplying the cylindrical div operator on both sides of Equation (28), then we have

$$(\lambda + 2\mu) \nabla^2 e - \beta_1 \nabla^2 \theta - \beta_2 \nabla^2 C = \rho \frac{\partial^2 e}{\partial t^2} \tag{29}$$

By using the following dimensionless quantities, the control equations can be more conveniently put into practice:

$$\begin{aligned} (r', u') &= c_1 \eta(r, u), \quad (t', \tau'_0, \tau'_1) = c_1^2 \eta(t', \tau_0, \tau_1), \\ \theta' &= \frac{\beta_1}{\lambda+2\mu} \theta, \quad P' = \frac{P}{\beta_2}, \quad C' = \frac{\beta_2}{\lambda+2\mu} C, \\ \sigma'_{ij} &= \frac{1}{\lambda+2\mu} \sigma_{ij}, \quad \eta = \frac{\rho C_E}{K}, \quad c_1^2 = \frac{\lambda+2\mu}{\rho} \end{aligned} \tag{30}$$

Equations (22)–(26) and (29) in the non-dimensional variables can be expressed as follows:

$$\nabla^2 e - \nabla^2 \theta - \nabla^2 C = \frac{\partial^2 e}{\partial t^2} \tag{31}$$

$$\frac{\partial^2}{\partial t^2} \left(1 + \tau_0 \frac{\partial}{\partial t} \right) [\theta + \varepsilon e + \eta_1 C] = \left(\frac{\partial}{\partial t} + \gamma_1 \right) \nabla^2 \theta \tag{32}$$

$$\left(\frac{\partial}{\partial t} + \frac{D^*}{\beta_2 D} \right) (\eta_3 \nabla^2 C - \nabla^2 e - \eta_4 \nabla^2 \theta) = \eta_2 \left(1 + \tau_1 \frac{\partial}{\partial t} \right) \frac{\partial^2 C}{\partial t^2} \tag{33}$$

$$\sigma_{rr} = (1 - 2\beta^2) e + 2\beta^2 \frac{\partial u}{\partial r} - \theta - C \tag{34}$$

$$\sigma_{\Theta\Theta} = (1 - 2\beta^2) e + 2\beta^2 \frac{u}{r} - \theta - C \tag{35}$$

$$P = \eta_3 C - e - \eta_4 \theta \tag{36}$$

where

$$\begin{aligned} \eta_1 &= \frac{a\beta_1 T_0}{\eta K \beta_2}, \quad \eta_4 = \frac{a\rho c_1^2}{\beta_1 \beta_2}, \quad \eta_2 = \frac{\rho c_1^2}{\beta_2^2 \eta D}, \quad \eta_3 = \frac{b\rho c_1^2}{\beta_2^2}, \\ \varepsilon &= \frac{\beta_1^2 T_0}{\rho^2 c_E c_1^2}, \quad \gamma_1 = \frac{K^*}{\rho C_E K}, \quad \beta^2 = \frac{\mu}{\lambda+2\mu}, \quad \gamma_2 = \frac{D^*}{\beta_2 D} \end{aligned} \tag{37}$$

We have lowered the primes for simplicity in Equations (31)–(36).

4. Initial and Boundary Conditions

The initial conditions can be assumed as

$$u = 0 = \frac{\partial u}{\partial t}, \quad \theta = 0 = \frac{\partial \theta}{\partial t}, \quad C = 0 = \frac{\partial C}{\partial t}, \quad t = 0 \tag{38}$$

The following boundary conditions can be considered

$$\sigma_{rr} = 0 \quad \text{at} \quad r = R \tag{39}$$

$$\theta = \theta_0 t e^{-t/2} \cos(t) \quad \text{at} \quad r = R \tag{40}$$

$$P = P_0 H(t) \quad \text{at} \quad r = R \tag{41}$$

where θ_0 and P_0 are constants, and $H(t)$ is the Heaviside unit step function.

5. Solution in the Laplace Transform Domain

Applying the Laplace transform to Equations (31)–(36) under the initial conditions (38), described by

$$\bar{f}(r, s) = \int_0^\infty e^{-st} f(r, t) dt \tag{42}$$

we obtain

$$(\nabla^2 - s^2) \bar{e} = \nabla^2 \bar{\theta} + \nabla^2 \bar{C} \tag{43}$$

$$\varepsilon \bar{\zeta}_1 \bar{e} + \eta_1 \bar{\zeta}_1 \bar{C} = (\nabla^2 - \bar{\zeta}_1) \bar{\theta} \tag{44}$$

$$(\eta_3 \nabla^2 - \bar{\zeta}_2) \bar{C} = \nabla^2 \bar{e} + \eta_4 \nabla^2 \bar{\theta} \tag{45}$$

$$\bar{\sigma}_{rr} = (1 - 2\beta^2)\bar{e} + 2\beta^2\frac{d\bar{u}}{dr} - \bar{\theta} - \bar{C} \tag{46}$$

$$\bar{\sigma}_{\theta\theta} = (1 - 2\beta^2)\bar{e} + 2\beta^2\frac{\bar{u}}{r} - \bar{\theta} - \bar{C} \tag{47}$$

$$P = \eta_3\bar{C} - e - \eta_4\bar{\theta} \tag{48}$$

where

$$\zeta_1 = \frac{s^2(1 + \tau_0s)}{s + \gamma_1}, \zeta_2 = \frac{\eta_2s^2(1 + \tau_1s)}{s + \gamma_2} \tag{49}$$

Eliminating \bar{e}, \bar{C} between Equations (43)–(45), we obtain

$$\left(\nabla^6 - \Lambda_1\nabla^4 + \Lambda_2\nabla^2 - \Lambda_3\right)\bar{\theta} = 0 \tag{50}$$

where

$$\begin{aligned} \Lambda_1 &= \frac{y_3x_1 + y_2 + y_1x_3 - x_2}{y_1 - x_1}, \Lambda_2 = \frac{x_2y_3 - y_2x_3 + y_1x_4}{y_1 - x_1}, \Lambda_3 = \frac{x_4y_2}{y_1 - x_1} \\ x_1 &= \frac{\zeta_1(\epsilon\eta_3 + \eta_1)}{\eta_3}, x_2 = \frac{\epsilon\zeta_1\zeta_2}{\eta_3}, x_3 = \frac{\zeta_2 + \eta_3\zeta_1 + \eta_1\eta_4\zeta_1}{\eta_3}, x_4 = \frac{\zeta_1\zeta_2}{\eta_3} \\ y_1 &= \zeta_1(\epsilon + \eta_1), y_2 = s^2\eta_1\zeta_1, y_3 = \zeta_1(\eta_1 - 1) \end{aligned} \tag{51}$$

By the same manner, we can demonstrate that the functions \bar{e} and \bar{C} can fulfill the equations

$$\left(\nabla^6 - \Lambda_1\nabla^4 + \Lambda_2\nabla^2 - \Lambda_3\right)\bar{e} = 0 \tag{52}$$

$$\left(\nabla^6 - \Lambda_1\nabla^4 + \Lambda_2\nabla^2 - \Lambda_3\right)\bar{C} = 0 \tag{53}$$

Introducing the parameters m_i ($i = 1, 2$) into Equation (50), we have

$$\left(\nabla^2 - m_1^2\right)\left(\nabla^2 - m_2^2\right)\left(\nabla^2 - m_3^2\right)\bar{\theta} = 0 \tag{54}$$

where m_1^2, m_2^2 and m_3^2 are the solutions for the equation:

$$m^6 - \Lambda_1m^4 + \Lambda_2m^2 + \Lambda_3 = 0 \tag{55}$$

The parameters m_1, m_2 and m_3 can be determined as

$$\begin{aligned} m_1 &= \sqrt{\frac{1}{3}[2p \sin(q) + A_1]}, \quad m_2 = \sqrt{-\frac{p}{3}\left[\sqrt{3} \cos(q) + \sin(q)\right] + \frac{A_1}{3}}, \\ m_3 &= \sqrt{\frac{p}{3}\left[\sqrt{3} \cos(q) - \sin(q)\right] + \frac{A_1}{3}}, \quad p = \sqrt{A_1^2 - 3A_2}, \\ q &= \frac{1}{3} \sin^{-1}(\chi), \quad \chi = -\frac{2A_1^3 - 9A_1A_2 + 27A_3}{2p^3}. \end{aligned} \tag{56}$$

The solution of Equation (54), which is infinitely limited, is given by

$$\bar{\theta}(r, s) = \sum_{i=1}^3 B_i(s)K_0(m_i r) \tag{57}$$

where B_i , ($i = 1, 2, 3$) are the integral parameters and $K_{1/2}(\cdot)$ denotes the second kind of Modified Bessel function of zero order. Likewise, we can write

$$\bar{e}(r, s) = \sum_{i=1}^3 B'_i(s)K_0(m_i r) \tag{58}$$

$$\bar{C}(r, s) = \sum_{i=1}^3 B''_i(s)K_0(m_i r) \tag{59}$$

Inserting Equations (58) and (59) into Equations (43)–(45), the following relations can be obtained

$$B'_i = \frac{m_i^4 + y_3 m_i^2}{y_1 m_i^2 - y_2} B_i = \Gamma_i B_i, B''_i = \frac{m_i^2(1 - \Gamma_i) - s^2}{m_i^2} B_i = \Omega_i B_i \tag{60}$$

Then, Equations (58) and (59) may be expressed as

$$\bar{e}(r, s) = \sum_{i=1}^3 \Gamma_i B_i K_0(m_i r) \tag{61}$$

$$\bar{C}(r, s) = \sum_{i=1}^3 \Omega_i B_i K_0(m_i r) \tag{62}$$

After using the relationship between \bar{u} and \bar{e} , the solution of the radial displacement \bar{u} will be

$$\bar{u}(r, s) = - \sum_{i=1}^3 \frac{\Gamma_i}{m_i} B_i(s) K_1(m_i r) \tag{63}$$

Using the expressions (57), (61)–(63) and the well-known relation

$$xK'_n(x) = -xK_{n-1}(x) - nK_n(x) \tag{64}$$

we can obtain the solutions of the thermal stresses and the chemical potential as

$$\bar{\sigma}_{rr}(r, s) = \sum_{i=1}^3 \left((\Gamma_i - 1 - \Omega_i) K_0(m_i r) + \frac{2\Gamma_i \beta^2}{m_i r} K_1(m_i r) \right) B_i \tag{65}$$

$$\bar{\sigma}_{\theta\theta}(r, s) = \sum_{i=1}^3 \left(\left((1 - 2\beta^2) \Gamma_i - 1 - \Omega_i \right) K_0(m_i r) - \frac{2\Gamma_i \beta^2}{m_i r} K_1(m_i r) \right) B_i \tag{66}$$

$$\bar{P}(r, s) = \sum_{i=1}^3 (\eta_3 \Omega_i - \eta_4 - \Gamma_i) K_0(m_i r) B_i \tag{67}$$

The boundary conditions in Equations (39)–(41) at $r = R$ in the transformed domain may be expressed as

$$\bar{\sigma}_{rr}(R, s) = 0, \quad \bar{\theta}(R, s) = \frac{4\theta_0(-3 + 4s + 4s^2)}{(5 + 4s + 4s^2)^2} = M(s), \quad \bar{P}(R, s) = \frac{P_0}{s} \tag{68}$$

Using the boundary conditions (68) with Equations (57), (65), and (67), the following linear system of equations can be obtained:

$$\sum_{i=1}^3 B_i(s) K_0(m_i r) = M(s) \tag{69}$$

$$\sum_{i=1}^3 \left((\Gamma_i - 1 - \Omega_i) K_0(m_i r) + \frac{2\Gamma_i \beta^2}{m_i r} K_1(m_i r) \right) B_i = 0 \tag{70}$$

$$\sum_{i=1}^3 (\eta_3 \Omega_i - \eta_4 - \Gamma_i) K_0(m_i r) B_i = \frac{P_0}{s} \tag{71}$$

The unknown parameters $B_1, B_2,$ and B_3 can be determined by resolving the system (69)–(71). By the setting of the constants $B_1, B_2,$ and B_3 and substitution in the general solutions of the different functions, this means that we have finished solving the problem in the field of the Laplace Transform.

5.1. Generalized MGT Model of Thermoelasticity without DIFFUSION

In this case, we take $C = P = 0$. However, the functions $\bar{\theta}$ and \bar{e} may be obtained Laplace transform domain by solving the two differential equations:

$$(\nabla^2 - s^2)\bar{e} = \nabla^2\bar{\theta} \tag{72}$$

$$\varepsilon\zeta_1\bar{e} = (\nabla^2 - \zeta_1)\bar{\theta} \tag{73}$$

Eliminating $\bar{e}(r, s)$ or $\bar{\theta}(r, s)$ in the above equation, one obtains the fourth-order differential equation:

$$(\nabla^4 - E_1\nabla^2 + E_2)\{\bar{\theta}, \bar{e}\} = 0 \tag{74}$$

where

$$E_1 = s^2 + \zeta_1(\varepsilon + 1), E_2 = s^2\zeta_1 \tag{75}$$

The solutions to Equation (55) are given by

$$\bar{\theta}(r, s) = \sum_{i=1}^2 K_0(m_i r)G_i(s) \tag{76}$$

$$\bar{e}(r, s) = \sum_{i=1}^2 H_i K_0(m_i r)G_i(s) \tag{77}$$

where $H_i = \frac{n_i^2 - \zeta_1}{\varepsilon\zeta_1}$, G_i ($i = 1, 2$) are integral constants and n_i^2 are given by

$$n_j^2 = \frac{1}{2} \left(E_1 \pm \sqrt{E_1^2 - 4E_2} \right) \tag{78}$$

Based on these solutions, the quantities of other physical fields can be simplified in the same way as in the previous analysis:

$$\bar{u}(r, s) = - \sum_{i=1}^2 \frac{H_i}{m_i} K_1(n_i r)G_i(s) \tag{79}$$

$$\bar{\sigma}_{rr}(r, s) = \sum_{i=1}^2 \left((H_i - 1)K_0(n_i r) + \frac{2H_i\beta^2}{m_i r} K_1(n_i r) \right) B_i \tag{80}$$

$$\bar{\sigma}_{\theta\theta}(r, s) = \sum_{i=1}^2 \left(\left((1 - 2\beta^2)H_i - 1 \right) K_0(n_i r) - \frac{2H_i\beta^2}{m_i r} K_1(n_i r) \right) B_i \tag{81}$$

To complete the solution in this case, the boundary conditions in Equations (39) and (40) are sufficient to obtain the integral constants G_i ($i = 1, 2$).

5.2. Special Cases of Thermoelasticity and Thermo-Diffusion Models

The model and equations derived and obtained in the second section of this paper are valid for many special cases that can be inferred from our constructed model. A system of equations containing thermal conduction equation (Equation (15)) and diffusion equation (Equation (16)) may include at least 10 generalized theories of thermal elasticity in the absence of diffusion as well as some generalized diffusion theories. The following can be summarized and documented in some special cases:

Case I: When the diffusion effect is absent

If the diffusion effect is missing ($C = 0$), it is possible to obtain the following models:

- The traditional theory of thermoelasticity (CTE) [1] when $K^* = \tau_0 = 0$.
- The Lord and Shulman generalized theory (LS) [2] by setting $K^* = 0$.

- The Green and Naghdi model of Type II (GN-II) [6] when the first term on the right-hand side of Equation (15) is disregarded and $\tau_0 = 0$.
- The Green and Naghdi theory of Type III (GN-III) [5] when $\tau_0 = 0$.
- The Moore–Gibson–Thompson thermoelasticity theory MGTE [15,17] when $K^*, \tau_0 > 0$.

Case II: Taking into account the effect of diffusion

- The conventional thermo-diffusion model (CTED) [33–35] when $K^* = \tau_0 = 0$.
- The generalized thermoelastic diffusion model (GTD) [36] by setting $K^* = 0$ and $D^* = 0$.
- The Green and Naghdi thermoelastic diffusion theory of Type II (GND-II) [49] when the first term on the right-hand side of Equation (15) is neglected with the addition of $D = \tau_0 = 0$.
- The Green and Naghdi thermoelastic diffusion theory of Type III (GND-III) [50] when thermal relaxation $\tau_0 = 0$.
- The Moore–Gibson–Thompson diffusion thermoelasticity theory MGTEd when the parameters $K^*, D^*, \tau_0 > 0$.

5.3. Inversion of the Laplace Transforms

Many problems have solutions that may be expressed in terms of a Laplace transform, which is therefore too difficult to invert using complex analysis techniques. The numerical evaluation of the Laplace inversion integral has been accomplished using a variety of approaches. Many papers have been written in the literature on the inversion of the Laplace transform. See, for example, [51–54], and a detailed bibliography can be found in [55,56].

Some methods work amazingly well with some image functions, while providing horrific results for others. Since no approach is best in all cases, we recommend using several alternative strategies to solve a particular reversal problem. We can be more confident and accept a numerically inverse Laplace transform if two or more methods give approximately the same result. In [57], Abate and Valkó have classified those algorithms into four categories according to the basic approach of the method as follows: (1) Fourier series expansion; (2) Laguerre function expansion; (3) combination of Gaver functionals; (4) deform the Bromwich contour.

This work presents the numerical inversion technique of Laplace transforms based on the Durbin and Fourier series expansion [58] and Honig and Hirdes [53]. The disadvantage of this type of inversion method, the remarkable dependence of estimation, and truncation error on free parameters is overcome by applying a procedure to reduce the estimation error, a method to speed up the Fourier series convergence, and a procedure that roughly computes the “best” option for all free parameters at the same time. For two reasons, this approach is effective in meeting the demands of standalone digital computing. Compared to other more complex numerical squaring methods, it is fast (economical) on the digital computers that are currently accessible. Second, because the inverse function is given as a Fourier cosine series with the coefficients being acceptable forward transform values, the technique is theoretically straightforward and requires minimal programming effort.

The Laplace transform and its inversion formula of the function $f(t)$ are defined as follows:

$$F(r, s) = \int_0^{\infty} e^{-st} f(r, t) dt \quad (82)$$

$$f(r, t) = \frac{1}{2\pi i} \int_{\vartheta - i\infty}^{\vartheta + i\infty} e^{st} F(r, s) ds \quad (83)$$

where $\vartheta > 0$ is arbitrary but must be chosen so that it is greater than the real parts of all the singularities of $F(r, s)$. For purposes of discussion, it is herein assumed that these integrals exist for $\text{Re}(s) > \vartheta > 0$. Using the inversion formula

$$f(r, t) = \frac{e^{\vartheta t}}{\pi} \int_0^{\infty} [\text{Re}\{F(r, s)\} \cos(\omega t) - \text{Im}\{F(r, s)\} \sin(\omega t)] d\omega, \quad (84)$$

which is equivalent to (2) with $s = \vartheta + iw$, $\vartheta, w \in \mathbb{R}$, and a Fourier series expansion of $e^{-\vartheta t} f(r, t)$ in the interval $[0, 2t_1]$, Durbin derived the approximation formula

$$f(r, t) \cong \frac{2e^{\vartheta t}}{t_1} \left(\frac{1}{2} \operatorname{Re} F(r, \vartheta) + \operatorname{Re} \sum_{N=1}^{\infty} F \left(r, \vartheta + \frac{iN\pi}{t_1} \right) \cos \left(\frac{N\pi}{t_1} t \right) \right) \quad (85)$$

where the parameter N is a satisfactorily large integer and denotes the number of stops in the truncated Fourier series. The parameter N can be chosen so that it is

$$e^{\vartheta t} \operatorname{Re} \left(e^{iN\pi t/t_1} g(c + iN\pi/t_1) \right) \leq \varepsilon_1 \quad (86)$$

where ε_1 is a persecuted small positive number that corresponds to the degree of accuracy to be achieved. A good choice of free parameters N and ϑt is important not only for the accuracy of the results but also for the application of the “Korrektur” method and convergence acceleration methods. These methods do not improve results if the parameters are badly chosen. For faster convergence, numerical experiments have shown that the value of the parameter ϑ that satisfies the above relation is given in terms of time as $\vartheta \approx 4.7/t$ [13].

6. Numerical Example and Discussion

We will now present some empirical results numerically to explain the new model introduced in this work and on the basis of preceding section outcomes. In order to answer the issue more comprehensively and to see how the studied fields depend on diffusion and certain physical influences, we have also numerically calculated for a particular physical material. The physical values of copper were selected for the purpose of mathematical estimation. The properties of this substance are therefore given in the SI units as follows [39,40]:

$$\begin{aligned} T_0 &= 293\text{K}, \rho = 8954\text{kgm}^{-3}, \tau_0 = 0.02\text{s}, \alpha_1 = 0.06\text{s}, C_E = 383.1\text{Jkg}^{-1}\text{K}^{-1} \\ \alpha_2 &= 0.09\text{s}, \alpha_t = 1.78 \times 10^{-5}\text{K}^{-1}, \alpha_c = 1.98 \times 10^{-4}\text{m}^3\text{kg}^{-1} \\ \{\mu, \lambda\} &= \{3.86, 7.76\} \times 10^{10}\text{kgm}^{-1}\text{s}^{-2}, \tau_1 = 0.2\text{s}, b = 0.9 \times 10^6\text{m}^5\text{kg}^{-1}\text{s}^{-2} \\ \alpha &= 1.2 \times 10^4\text{m}^2\text{s}^{-2}\text{K}^{-1}, K = 386\text{Wm}^{-1}\text{K}^{-1}, D = 0.85 \times 10^{-8}\text{kgsm}^{-3} \end{aligned} \quad (87)$$

All of the parameters calculated $t = 0.12$, $\gamma_1 = 1$ and $\gamma_2 = 0.5$ will be used in calculations unless are determined otherwise. The numerical procedure defined in (84) has been applied to obtain the temperature θ , displacement u , radial stress σ_{rr} , hoop stress $\sigma_{\theta\theta}$, and concentration C as the chemical potential P distributions within the medium. We assume that the cylinder cavity, with its center, has a radius of $R = 1$ from the origin.

By comparing the basic Green and Naghdi theories of the second and third types with the modified thermal diffusion model, this section will provide some examples and applications for testing the validity of the given model. Plot activities are seen in the hollows cylinder’s radial pathway. The tabulation of some of the results for future comparisons to other researchers is an important part of this study.

The effects of the field variables analyzed based on the thermo-diffusion theories CTED, CTED, GND-II, GND-III, and MGTED have been reported in Tables 1–6. In the radial direction of the cylinder, Figures 1–6 display further sample graphs of all models to assess the effect of various thermal diffusion models on the quantities of the physical fields.

In the presence of the diffusion effect, Table 1 and Figure 1 display the variance of the temperature vs. the radial distance r for the different theories. The temperature values θ reach the maximum values on the surface of the spherical cavity $r = 1$ as shown in the table and the figure, and then gradually decrease. The distribution of temperature satisfies the condition of the thermal boundary imposed upon the problem. The values of θ gradually decrease and ultimately decrease in the opposite direction of the heat-wave propagation to a value of zero as the radius r increases.

Table 1. The temperature θ for different thermo-diffusion models.

r	CTED	CTED	GND-II	GND-III	MGTED
1.0	0.482375	0.482375	0.482375	0.482375	0.482375
1.2	0.295083	0.243376	0.277035	0.308172	0.258926
1.4	0.182314	0.123602	0.160531	0.198940	0.140311
1.6	0.113203	0.0625852	0.0932805	0.129202	0.0762489
1.8	0.0703235	0.0311688	0.0540023	0.084112	0.0412362
2.0	0.0434885	0.0149006	0.0308823	0.0546925	0.0219489
2.2	0.0265966	0.00647244	0.0172123	0.0353729	0.0112778
2.4	0.0159271	0.0021343	0.00912002	0.0226299	0.00537005
2.6	0.00918038	5.9651×10^{-5}	0.00434163	0.0142029	0.00211293
2.8	0.00492057	1.1276×10^{-5}	0.0015413	0.00862565	0.000337224
3.0	0.00224365	1.6055×10^{-5}	0.000075166	0.00493878	0.000608679

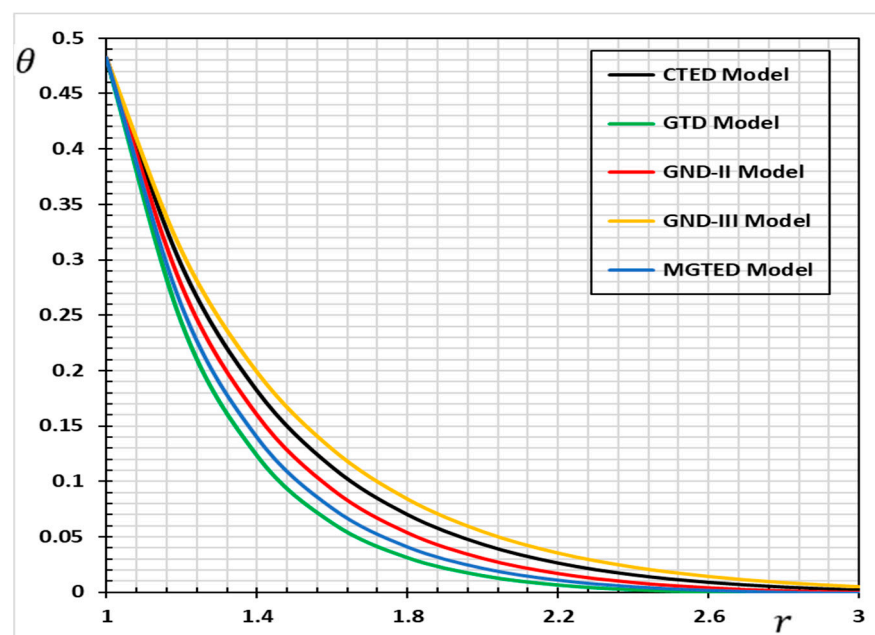


Figure 1. The temperature θ for different thermo-diffusion models.

A great difference in the temperature field has been found near the boundary surface of the body under all thermo-diffusion theories, considering the convergence of all models when increasing the radius within the body. It was also noted that in the CTED and GND-III models, higher temperature values were observed compared to the GN-II, GTD, and MGTED models. In the CTED and GND-III models, thermal waves do not fade easily, unlike in other thermal diffusion models in which it is clear that thermal waves spread at slow speeds inside the medium. This is because the heat waves in the CTED model propagate at an unlimited velocity. It is also noted that in the case of the MGTED model, the numerical values are lower inside the body away from the spherical cavity of the surface than in the case of the GND-III model, and the waves also fade away faster. The explanation for the rapid decrease, as predicted, is the inclusion of relaxation times in the equations extracted.

The effect of all thermal diffusion models on the displacement u in the radial direction of the cylinder is shown in Table 2 and Figure 2. The displacement distribution begins at a negative value and then increases gradually as the distance increases until it reaches a peak value of approximately $r = 1.2$, after which it eventually decreases to zero with r increasing. From the table and figure, it can be seen that the relaxation times τ_0 and τ_1 that were used in the current thermo-diffusion model have a significant role to play in body deformation.

Table 2. The displacement u for different thermo-diffusion models.

r	CTED	CTED	GND-II	GND-III	MGTED
1.0	−0.079734	−0.081456	−0.099797	−0.099287	−0.074101
1.2	0.00409436	0.00133869	0.00216732	0.00452298	0.00362599
1.4	0.00905289	0.00598837	0.00779358	0.0106263	0.00823209
1.6	0.00538761	0.00330092	0.00482924	0.00685372	0.00474181
1.8	0.00287224	0.00167184	0.00275236	0.00392333	0.00246476
2.0	0.00160078	0.000948539	0.00169206	0.00228376	0.0013645
2.2	0.00098475	0.000627214	0.00115203	0.00141395	0.000850296
2.4	0.000674483	0.000465978	0.00085086	0.000945582	0.000595687
2.6	0.000504701	0.000370188	0.000662123	0.000681815	0.000455172
2.8	0.000401442	0.000304314	0.000531199	0.000523657	0.000367178
3.0	0.000331688	0.000254552	0.00043369	0.000421697	0.000305562

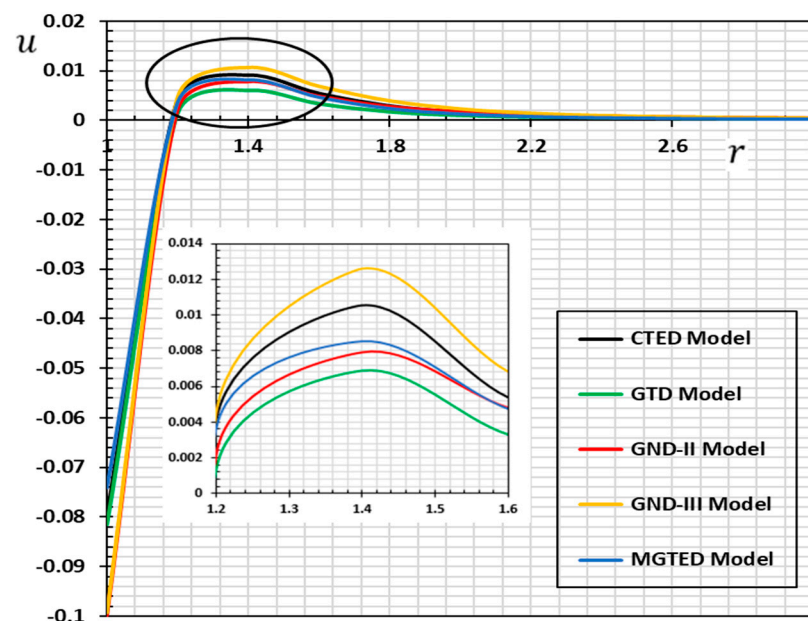


Figure 2. The displacement u for different thermo-diffusion models.

In the case of modified GTD, GND-II, and modified MGTED models, numerical values of disolactivity are also smaller compared to the findings of the CTED and GN-III models. In general, it seems that in various theories, there is great similarity and convergence in the action of displacement. Only in magnitude and peak points does the difference arise. It can be detected that when relaxation times are used, the displacement profile for the Green and Naghdi thermo-diffusion model (GND-III) is greater in the absence of relaxation times than for the MGTED thermo-diffusion model.

For various combinations of thermo-diffusion models, Tables 3 and 4 and Figures 3 and 4 are provided to investigate the effect of thermo-diffusion on the variance of thermal stresses σ_{rr} and $\sigma_{\theta\theta}$. The comparison between the various models and the various distributions of heat stress can be observed. It is also noted that, in comparison to the CTED model, the magnitudes of stress values in the case of thermal diffusion GN-III models are the largest possible.

Table 3. The radial stress σ_{rr} for different thermo-diffusion models.

r	CTED	CTED	GND-II	GND-III	MGTED
1.0	0	0	0	0	0
1.2	-0.854538	-0.363519	-0.612671	-1.0998	-0.506898
1.4	-0.426424	-0.150462	-0.280248	-0.584935	-0.242656
1.6	-0.225884	-0.0670708	-0.137284	-0.326984	-0.124743
1.8	-0.123914	-0.0310105	-0.0697059	-0.189105	-0.0664459
2.0	-0.0694617	-0.0146615	-0.0361796	-0.111722	-0.0361722
2.2	-0.0395136	-0.00703726	-0.0190601	-0.0669692	-0.0199845
2.4	-0.0227178	-0.0034148	-0.01015	-0.0405677	-0.0111598
2.6	-0.0131671	-0.00167074	-0.00544939	-0.0247716	-0.00628256
2.8	-0.00768002	-0.000822742	-0.0029445	-0.0152214	-0.00355943
3.0	-0.00450248	-0.000407266	-0.00159924	-0.0094005	-0.00202698

Table 4. The hoop stress $\sigma_{\theta\theta}$ for different thermo-diffusion models.

r	CTED	CTED	GND-II	GND-III	MGTED
1.0	-0.372282	-0.376351	-0.372118	-0.373018	-0.37111
1.2	-0.852663	-0.362632	-0.611177	-1.09758	-0.505897
1.4	-0.426185	-0.150271	-0.280019	-0.584682	-0.242504
1.6	-0.225779	-0.0669935	-0.137185	-0.326875	-0.124674
1.8	-0.12386	-0.0309766	-0.0696585	-0.189046	-0.0664112
2.0	-0.0694327	-0.014646	-0.0361559	-0.111689	-0.036154
2.2	-0.0394976	-0.00702998	-0.0190479	-0.0669499	-0.0199748
2.4	-0.0227088	-0.00341133	-0.0101436	-0.0405563	-0.0111544
2.6	-0.0131619	-0.00166907	-0.00544603	-0.0247648	-0.00627961
2.8	-0.00767706	-0.000821926	-0.0029427	-0.0152172	-0.00355778
3.0	-0.00450077	-0.000406865	-0.00159828	-0.00939798	-0.00202605

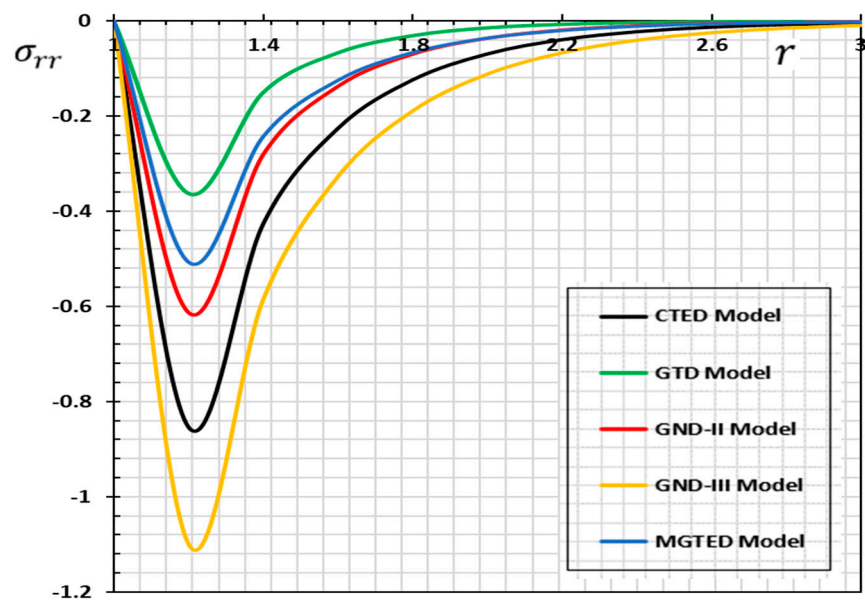


Figure 3. The radial stress σ_{rr} for different thermo-diffusion models.

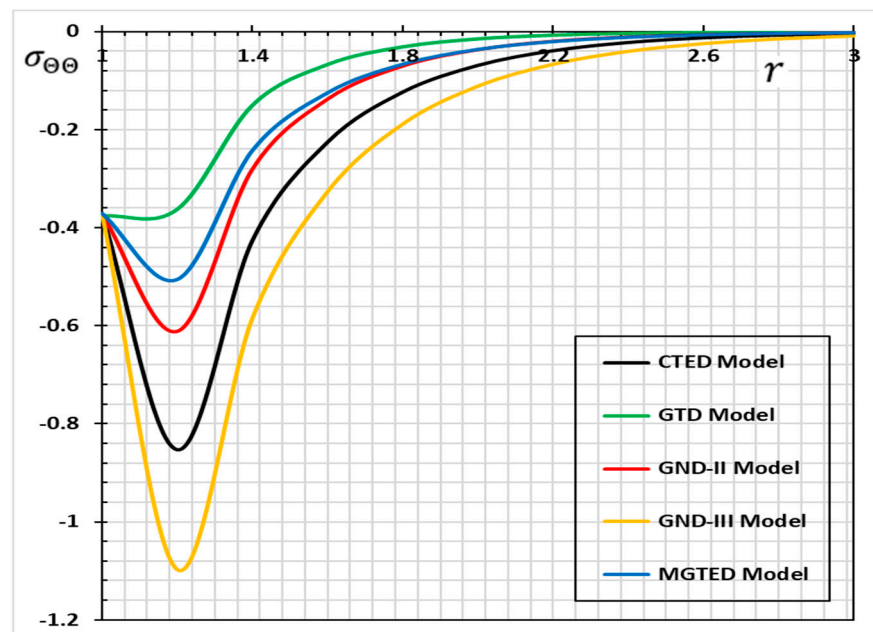


Figure 4. The hoop stress $\sigma_{\theta\theta}$ for different thermo-diffusion models.

The radial thermal stress σ_{rr} starts at zero, filling the conditions of the proposed problem, then decreases rapidly until at the peak point it reaches its maximum value, and then decreases steadily until it disappears to zero (see Table 3 and Figure 3). With the hoop stress $\sigma_{\theta\theta}$, the same previous behavior occurs except that it starts with a negative value different from zero at the surface of the spherical cavity. In behavior and principles, the variations in GTD-, GND-II-, and MGTED-generalized thermal diffusion models are similar together.

The existence of the relaxation parameters of generalized thermoelasticity (GND-III) and the diffusion that have been integrated into the current model (MGTED) have a major effect on the properties and actions of the vibrations of the different distributions.

It can be attributed to the compressive essence of stress that atoms are suppressed together in the solids and voluminosly induce compressive stress because of the dissolution of the substance. In both cases, the comparison of each figure shows that, as time pass away from the source, the magnitude of the various quantities considered decreases, thus showing the wave fronts.

For the five separate thermo-diffusion models, the numerical computations of the chemical potential P against the radial distance r are shown graphically in Figure 5 and in Table 5. Figure 5 and Table 5 show that at the beginning, the variance of the chemical potential P is great and that the vibrations of the transition decrease and fade as the r value increases. The chemical potential P profile has also been established, starting with the greatest surface value, meeting the boundary conditions imposed on the problem, and this confirms and validates the outcomes we have obtained. In Figure 5 and Table 5, we note that the variations in the case of CEDT and GND-III are similar to each other and have the highest values, while the GTD models GND-II and MGTED are smaller in size due to the effect of generalized thermal and diffusion relaxation parameters.

The comparison with space for the distribution of concentration C is shown in Figure 6 and Table 6 for different thermos-diffusion models. From the numerical values, it was found that there were some variations between the values of concentration C and the variation in the model. The concentration C curves and tables have the same behavior but vary only in quantity.

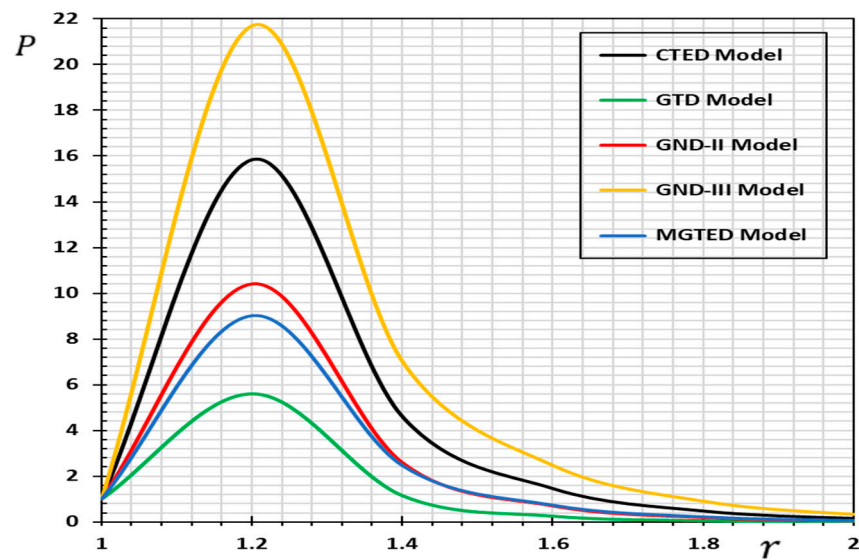


Figure 5. The chemical potential P for different thermo-diffusion models.

Table 5. The chemical potential P for different thermo-diffusion models.

r	CTED	CTED	GND-II	GND-III	MGTED
1.0	1.013155	1.013155	1.013155	1.013155	1.013155
1.2	15.8287	5.60381	10.4178	21.6918	9.01363
1.4	4.60106	1.15509	2.59169	7.01602	2.46841
1.6	1.4672	0.262133	0.708675	2.48466	0.742418
1.8	0.488918	0.062235	0.202616	0.919069	0.233397
2.0	0.167186	0.0151707	0.0594624	0.348776	0.0753026
2.2	0.0581515	0.0037628	0.0177532	0.134612	0.0247144
2.4	0.0204726	0.000944823	0.00536546	0.0525816	0.00821032
2.6	0.0072729	0.000239424	0.00163639	0.0207244	0.00275235
2.8	0.00260187	6.11038×10^{-5}	0.00050261	0.00822539	0.000929177
3.0	0.000936034	1.56829×10^{-5}	0.000155245	0.00328282	0.000315449

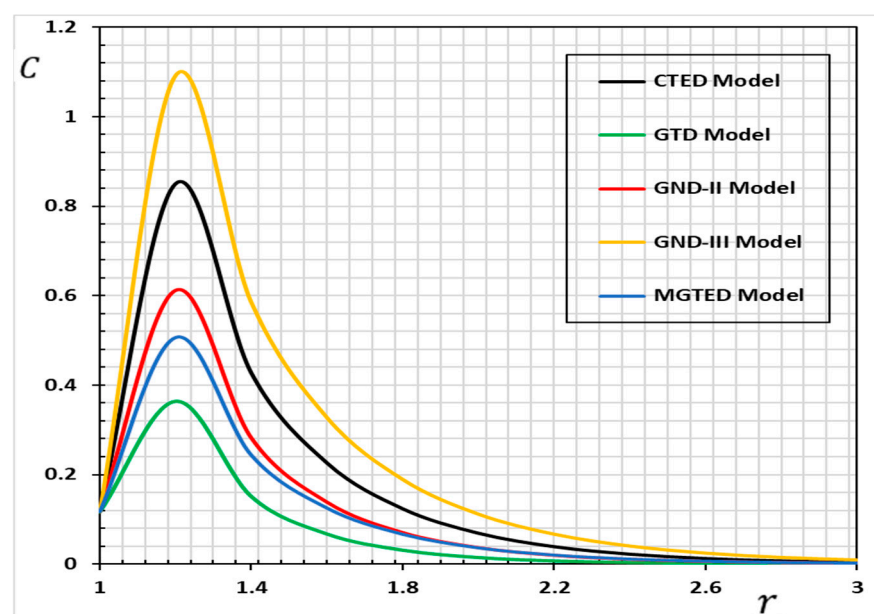


Figure 6. The concentration C for different thermo-diffusion models.

Table 6. The concentration C for different thermo-diffusion models.

r	CTED	CTED	GND-II	GND-III	MGTED
1.0	0.117031	0.116954	0.117034	0.117017	0.117052
1.2	0.850402	0.364377	0.611294	1.09261	0.506495
1.4	0.427816	0.151386	0.281513	0.58636	0.243597
1.6	0.226681	0.0674881	0.137925	0.327908	0.125236
1.8	0.124353	0.0312044	0.0700328	0.189644	0.0667094
2.0	0.0697087	0.0147534	0.0363497	0.112041	0.0363159
2.2	0.0396543	0.00708146	0.0191498	0.0671608	0.0200641
2.4	0.0227988	0.00343627	0.0101978	0.0406839	0.0112042
2.6	0.0132141	0.00168126	0.0054751	0.0248426	0.00630761
2.8	0.00770743	0.000827926	0.0029584	0.015265	0.00357363
3.0	0.00451856	0.000409833	0.00160679	0.00942747	0.00203507

The concentration begins with a positive value at the cavity of the cylinder and then rises steadily until $r = 1.2$ reaches its highest local maximum value. After that, increasing the distance r within the medium steadily decreases until it dissipates to obtain its null value. In contrast with the CTED and GND-III models, the C -field values can be inferred from the numeric values to be smaller in the case of the MGTEd model. The GND-III model, however, gives the GND-II model a larger model.

The medium is strained in the vicinity of the cylinder and, with the passing of time, is greater. Cross-effects may result in the presence of tensile stress near the cavity surface due to temperature coupling, mass dissemination, and strain fields. Owing to these cross-effects, an additional accumulation of thermal stress arises from the thermal excitation. The primary difference between the GND-III model of thermoelastic diffusion and the MGTEd-based thermal conductivity equations of thermoelastic diffusion is the additional delay times τ_0 and τ_1 .

These relaxation times provide an additional diffusion and propagation mechanism in the governing equation for the dissipation effect. The delay time τ_0 is known to monitor the propagation behavior of the thermal wave, slow down the speed of heat-wave propagation, and show the characteristics of the thermal wave. Thermal energy can be diffused, and diffusion wave decay characters can be produced in the MGTEd heat transfer by the τ_1 effect.

7. Conclusions

A new generalized thermoelastic diffusion model has been derived in the present paper, connecting heat and mass flux in elastic materials. It is understood that, due to the coupling between temperature and mass diffusion as well as stress fields, thermoelastic diffusion takes place in a flexible solid material. Centered on the Moore–Gibson–Thompson equation, the constitutive equations, as well as the heat and mass diffusion equations, have been modified. The goal behind the implementation of this new model was to deal with the evident inconsistency between the infinite thermal and diffusion rates predicted by the classical theories of thermoelastic diffusion [1,33–35] and the energy dissipation model of Green and Naghdi (GN-III) [5]. In the constructed modified model, the laws of Fourier and Fick have also been improved to incorporate the time needed to speed up the heat wave and the time derivative of the diffusive mass flow.

The primary distinction between the thermoelastic diffusion model GND-III and the thermoelastic diffusion thermal conductivity equations based on MGTEd is the additional delay times τ_0 and τ_1 . These relaxation times provide an additional diffusion and propagation mechanism in the governing equation for the dissipation effect. The delay time τ_0 is known to monitor the propagation behavior of the thermal signal, slow down the speed of thermal wave propagation, and show the characteristics of the thermal wave.

Thermal energy can be diffused, and diffusion wave decay characters can be produced in the MGTEd heat transfer by the τ_1 effect.

The problem of an unbounded solid with a cylindrical cavity with a permeable material shaped on the surface in contact with the cylindrical cavity has been studied to explain and examine the proposed model. In the area of Laplace transformation, the solution is achieved by a direct approach. Centered on Fourier expansion techniques, a computational approach is used to invert Laplace transforms to solve the problem in the physical field.

It was found from our observations that thermal and diffusion waves are propagated as a wave with a slight velocity rather than an endless velocity on the conventional thermoelastic diffusion model. The thermoelastic diffusion models can be deduced as special cases: Green–Naghdi Type II and III models, generalized thermo-diffusion with one relaxation. Furthermore, the GND-III and CTED models have a near-conduct but are distinct from MGTEd, which shows that the model of thermoelastic diffusion was significant. The results in this article should be useful for science and engineering research as well as for those working on solid mechanics growth. A wide variety of thermodynamic concerns are related to the method used in this article. These theoretical conclusions will provide experimental experts and researchers who work on this subject with interesting knowledge.

Author Contributions: Conceptualization, Ö.C. and A.E.A.; methodology, A.E.A.; software, A.E.A.; validation, A.E.A. and H.E.; formal analysis, A.E.A.; investigation, A.E.A.; resources, A.E.A. and H.E.; data curation, H.E.; writing—original draft preparation, A.E.A. and H.E.; writing—review and editing, Ö.C. and H.E.; visualization, A.E.A. and H.E.; supervision, Ö.C.; project administration, Ö.C. and H.E.; funding acquisition, Ö.C. and H.E. All authors have read and agreed to the published version of the manuscript.

Funding: This research received no external funding.

Institutional Review Board Statement: Not applicable.

Informed Consent Statement: Not applicable.

Data Availability Statement: Not applicable.

Conflicts of Interest: The authors declare no conflict of interest.

References

1. Biot, M.A. Thermoelasticity and Irreversible Thermodynamics. *J. Appl. Phys.* **1956**, *27*, 240–253. [[CrossRef](#)]
2. Lord, H.; Shulman, Y. A generalized dynamical theory of thermoelasticity. *J. Mech. Phys. Solids* **1967**, *15*, 299–309. [[CrossRef](#)]
3. Green, A.E.; Lindsay, K.A. Thermoelasticity. *J. Elast.* **1972**, *2*, 1–7. [[CrossRef](#)]
4. Green, A.E.; Naghdi, P.M. A re-examination of the basic postulates of thermomechanics. *Proc. R. Soc. Lond. A* **1991**, *432*, 171–194. [[CrossRef](#)]
5. Green, A.E.; Naghdi, P.M. On undamped heat waves in an elastic solid. *J. Therm. Stress.* **1992**, *15*, 253–264. [[CrossRef](#)]
6. Green, A.E.; Naghdi, P.M. Thermoelasticity without energy dissipation. *J. Elast.* **1993**, *31*, 189–208. [[CrossRef](#)]
7. Choudhuri, S.K.R. On A Thermoelastic Three-Phase-Lag Model. *J. Therm. Stress.* **2007**, *30*, 231–238. [[CrossRef](#)]
8. Abouelregal, A.E. Modified fractional thermoelasticity model with multi-relaxation times of higher order: Application to spherical cavity exposed to a harmonic varying heat. *Waves Random Complex Media* **2019**, 1–21. [[CrossRef](#)]
9. Abouelregal, A.E. On Green and Naghdi thermoelasticity model without energy dissipation with higher order time differential and phase-lags. *J. Appl. Comput. Mech.* **2019**, *6*, 445–456.
10. Abouelregal, A.E. Two-temperature thermoelastic model without energy dissipation including higher order time-derivatives and two phase-lags. *Mater. Res. Express* **2019**, *6*, 116535. [[CrossRef](#)]
11. Abouelregal, A.E. A novel model of nonlocal thermoelasticity with time derivatives of higher order. *Math. Methods Appl. Sci.* **2020**, *43*, 6746–6760. [[CrossRef](#)]
12. Tzou, D.Y. A Unified Field Approach for Heat Conduction From Macro- to Micro-Scales. *J. Heat Transf.* **1995**, *117*, 8–16. [[CrossRef](#)]
13. Tzou, D.Y. *Macro-to Microscale Heat Transfer: The Lagging Behavior*, 1st ed.; Wiley: Hoboken, NJ, USA, 2014.
14. Dreher, M.; Quintanilla, R.; Racke, R. Ill-posed problems in thermomechanics. *Appl. Math. Lett.* **2009**, *22*, 1374–1379. [[CrossRef](#)]
15. Quintanilla, R. Moore-Gibson-Thompson thermoelasticity. *Math. Mech. Solids* **2019**, *24*, 4020–4031. [[CrossRef](#)]
16. Quintanilla, R. Moore-Gibson-Thompson thermoelasticity with two temperatures. *Appl. Eng. Sci.* **2020**, *1*, 100006. [[CrossRef](#)]
17. Abouelregal, A.E.; Ahmed, I.-E.; Nasr, M.E.; Khalil, K.M.; Zakria, A.; Mohammed, F.A. Thermoelastic Processes by a Continuous Heat Source Line in an Infinite Solid via Moore–Gibson–Thompson Thermoelasticity. *Materials* **2020**, *13*, 4463. [[CrossRef](#)] [[PubMed](#)]

18. Marin, M.; Othman, M.I.A.; Seadawy, A.R.; Carstea, C. A domain of influence in the Moore–Gibson–Thompson theory of dipolar bodies. *J. Taibah Univ. Sci.* **2020**, *14*, 653–660. [[CrossRef](#)]
19. Conti, M.; Pata, V.; Quintanilla, R. Thermoelasticity of Moore–Gibson–Thompson type with history dependence in the temperature. *Asymptot. Anal.* **2020**, *120*, 1–21. [[CrossRef](#)]
20. Aboueregail, A.E.; Sedighi, H.M. The effect of variable properties and rotation in a visco-thermoelastic orthotropic annular cylinder under the Moore–Gibson–Thompson heat conduction model. *Proc. Inst. Mech. Eng. Part L J. Mater. Des. Appl.* **2021**, *235*, 1004–1020. [[CrossRef](#)]
21. Fernández, J.R.; Quintanilla, R. Moore-Gibson-Thompson theory for thermoelastic dielectrics. *Appl. Math. Mech.* **2021**, *42*, 309–316. [[CrossRef](#)]
22. Aboueregail, A.E. An advanced model of thermoelasticity with higher-order memory-dependent derivatives and dual time-delay factors. *Wave. Random Complex Media* **2021**. [[CrossRef](#)]
23. Pellicer, M.; Quintanilla, R. On uniqueness and instability for some thermomechanical problems involving the Moore–Gibson–Thompson equation. *Zeitschrift für angewandte Mathematik und Physik* **2020**, *71*, 1–21. [[CrossRef](#)]
24. Abouelregail, A.E.; Moustapha, M.V.; Nofal, T.A.; Rashid, S.; Ahmad, H. Generalized thermoelasticity based on higher-order memory-dependent derivative with time delay. *Results Phys.* **2021**, *20*, 103705. [[CrossRef](#)]
25. Pellicer, M.; Solà-Morales, J. Optimal scalar products in the Moore-Gibson-Thompson equation. *Evol. Equ. Control Theory* **2019**, *8*, 203–220. [[CrossRef](#)]
26. Abouelregail, A.E.; Ahmad, H.; Yao, S.-W. Functionally Graded Piezoelectric Medium Exposed to a Movable Heat Flow Based on a Heat Equation with a Memory-Dependent Derivative. *Materials* **2020**, *13*, 3953. [[CrossRef](#)]
27. Bazarra, N.; Fernández, J.R.; Quintanilla, R. Analysis of a Moore-Gibson-Thompson thermoelastic problem. *J. Comput. Appl. Math.* **2021**, *382*, 113058. [[CrossRef](#)]
28. Dell’Oro, F.; Pata, V. On the Moore–Gibson–Thompson Equation and Its Relation to Linear Viscoelasticity. *Appl. Math. Optim.* **2016**, *76*, 641–655. [[CrossRef](#)]
29. Conti, M.; Pata, V.; Pellicer, M.; Quintanilla, R. On the analyticity of the MGT-viscoelastic plate with heat conduction. *J. Differ. Equ.* **2020**, *269*, 7862–7880. [[CrossRef](#)]
30. Singh, B.; Mukhopadhyay, S. Galerkin-type solution for the Moore–Gibson–Thompson thermoelasticity theory. *Acta Mech.* **2021**, *232*, 1273–1283. [[CrossRef](#)]
31. Kumar, R.; Kansal, T. Propagation of Lamb waves in transversely isotropic thermoelastic diffusive plate. *Int. J. Solids Struct.* **2008**, *45*, 5890–5913. [[CrossRef](#)]
32. Xiong, C.; Guo, Y. Electromagneto-thermoelastic diffusive plane waves in a half-space with variable material properties under fractional order thermoelastic diffusion. *Int. J. Appl. Electromagn. Mech.* **2017**, *53*, 251–269. [[CrossRef](#)]
33. Nowacki, W. Dynamical problems of thermodiffusion in solids. *Bull. Acad. Pol. Sci. Ser. Sci. Tech.* **1974**, *22*, 55–64.
34. Nowacki, W. Dynamical problems of thermodiffusion in solids II. *Bull. Acad. Pol. Sci. Ser. Sci. Tech.* **1974**, *22*, 129–135.
35. Nowacki, W. Dynamical problems of thermo diffusion in solid III. *Bull. Acad. Pol. Sci. Ser. Sci. Tech.* **1974**, *22*, 266–275.
36. Sherief, H.H.; Hamza, F.A.; Saleh, H.A. The theory of generalized thermoelastic diffusion. *Int. J. Eng. Sci.* **2004**, *42*, 591–608. [[CrossRef](#)]
37. Sherief, H.H.; Saleh, H.A. A half-space problem in the theory of generalized thermoelastic diffusion. *Int. J. Solids Struct.* **2005**, *42*, 4484–4493. [[CrossRef](#)]
38. Sherief, H.H.; El-Maghraby, N.M. A Thick Plate Problem in the Theory of Generalized Thermoelastic Diffusion. *Int. J. Thermophys.* **2009**, *30*, 2044–2057. [[CrossRef](#)]
39. Abouelregail, A.E. Generalized mathematical novel model of thermoelastic diffusion with four phase lags and higher-order time derivative. *Eur. Phys. J. Plus* **2020**, *135*, 1–21. [[CrossRef](#)]
40. Abouelregail, A.E.; Elhagary, M.A.; Soleiman, A.; Khalil, K.M. Generalized thermoelastic-diffusion model with higher-order fractional time-derivatives and four-phase-lags. *Mech. Based Des. Struct. Mach.* **2020**, 1–18. [[CrossRef](#)]
41. Kansal, T. Fundamental solution of the system of equations of pseudo oscillations in the theory of thermoelastic diffusion materials with double porosity. *Multidiscip. Model. Mater. Struct.* **2019**, *15*, 317–336. [[CrossRef](#)]
42. Abo-Dahab, S.M.; Abd-Alla, A.M. Dual-phase-lag model on magneto-thermoelastic rotating medium with voids and diffusion under the effect of initial stress and gravity. *Heat Transf.* **2020**, *49*, 2131–2166. [[CrossRef](#)]
43. Reddy, P.S.; Rao, V.P. Thermo-diffusion and diffusion-thermo effects on convective heat and mass transfer through a porous medium in a circular cylindrical annulus with quadratic density temperature variation-finite element study. *J. Appl. Fluid Mech.* **2012**, *5*, 139–144.
44. Paul, K.; Mukhopadhyay, B. A Generalized thermo-elastic diffusion problem in a functionally graded rotating media using fractional order theory. *J. Solid Mech.* **2020**, *12*, 263–277.
45. Giorgi, C.; Grandi, D.; Pata, V. On the Green-Naghdi Type III heat conduction model. *Discret. Contin. Dyn. Syst. B* **2014**, *19*, 2133–2143. [[CrossRef](#)]
46. Aouadi, M. Uniqueness and Reciprocity Theorems in the Theory of Generalized Thermoelastic Diffusion. *J. Therm. Stress.* **2007**, *30*, 665–678. [[CrossRef](#)]
47. Lasiecka, I.; Wang, X. Moore–Gibson–Thompson equation with memory, part II: General decay of energy. *J. Differ. Equ.* **2015**, *259*, 7610–7635. [[CrossRef](#)]

48. Lasiecka, I.; Wang, X. Moore–Gibson–Thompson equation with memory, part I: Exponential decay of energy. *Zeitschrift für Angewandte Mathematik und Physik* **2016**, *67*, 1–23. [[CrossRef](#)]
49. Aouadi, M.; Lazzari, B.; Nibbi, R. A theory of thermoelasticity with diffusion under Green–Naghdi models. *ZAMM* **2013**, *94*, 837–852. [[CrossRef](#)]
50. Lazzari, B.; Nibbi, R. Energy decay in Green–Naghdi thermoelasticity with diffusion and dissipative boundary controls. *J. Therm. Stress.* **2016**, *40*, 1–11. [[CrossRef](#)]
51. Kryzhniy, V.V. Numerical inversion of the Laplace transform: Analysis via regularized analytic continuation. *Inverse Probl.* **2006**, *22*, 579–597. [[CrossRef](#)]
52. Dong, C.W. A Regularization Method for the Numerical Inversion of the Laplace Transform. *SIAM J. Numer. Anal.* **1993**, *30*, 759–773. [[CrossRef](#)]
53. Honig, G.; Hirdes, U. A method for the numerical inversion of Laplace transforms. *J. Comput. Appl. Math.* **1984**, *10*, 113–132. [[CrossRef](#)]
54. Piessens, R.; Dang, N. A bibliography on numerical inversion of the laplace transform and applications: A supplement. *J. Comput. Appl. Math.* **1976**, *2*, 225–228. [[CrossRef](#)]
55. Narayanan, G.V.; Beskos, D.E. Numerical operational methods for time-dependent linear problems. *Int. J. Numer. Methods Eng.* **1982**, *18*, 1829–1854. [[CrossRef](#)]
56. Dubner, H.; Abate, J. Numerical inversion of Laplace transforms by relating them to the finite Fourier cosine transform. *J. Assoc. Comput. Mach.* **1968**, *15*, 115–123. [[CrossRef](#)]
57. Abate, J.; Valkó, P.P. Multi-precision Laplace transform inversion. *Int. J. Numer. Methods Eng.* **2004**, *60*, 979–993. [[CrossRef](#)]
58. Durbin, F. Numerical inversion of Laplace transforms: An effective improvement of Dubner and Abate’s method. *Comput. J.* **1973**, *17*, 371–376. [[CrossRef](#)]
59. Wan, D.C.; Patnaik, B.S.V.; Wei, G.W. A new benchmark quality solution for the buoyancy-driven cavity by discrete singular convolution. *Numer. Heat Transf. Part B Fundam.* **2001**, *40*, 199–228.
60. Zhou, Y.C.; Patnaik, B.S.V.; Wan, D.C.; Wei, G.W. DSC solution for flow in a staggered double lid driven cavity. *Int. J. Numer. Methods Eng.* **2003**, *57*, 211–234. [[CrossRef](#)]
61. Chernov, A.; Reinartz, A. Sparse grid approximation spaces for space–time boundary integral formulations of the heat equation. *Comput. Math. Appl.* **2019**, *78*, 3605–3619. [[CrossRef](#)]